LABORATORI NAZIONALI DI FRASCATI
SIS – Pubblicazioni

LNF-04/21 (IR)
15 ottobre 2004

LOCAL STRUCTURE PROPERTIES OF $Ga_{1-x}Al_xN$ EPITAXIAL LAYER

B.V.Robouch[1], A.Kisiel[2], E.Burattini[1] I.Kutcherenko[3], L.K.Vodopyanov[3]

[1)]INFN-Laboratori Nazionali di Frascati Via E. Fermi 40, I-00044 Frascati, Italy
[2)]Instytut Fizyki, Universytet Jagiellonski, Reymonta 4, 30-059 Krakow, Poland
[3)]P.N.Lebedev Physical Institute, Russian Academy of Science, Leninsky prospect 53, Moscow 119991, GSP-1
E-mails: robouch@lnf.infn.it kisiel@netmail.if.uj.edu.pl kucheren@sci.lebedev.ru

ABSTRACT

The *strained-tetrahedron* model is used to analyze the wurzite structure of epitaxial GaAlN thin films on a sapphire substrate. Site occupation preference (SOP) coefficients and first two shell inter-ion distances are calculated in the ideal wurzite structure approximation. The coefficient values W_1=0, W_2=1.86, and W_3=1, indicate a strong deviation from a random distribution with preference of Ga-N to Al-N pairs. This suggests that GaAlN thin films could be less homogeneous and more difficult to grow beyond 50% AlN. Also the far-infrared GaAlN phonon spectra should exhibit only four strong lines instead of eight.

PACS.: 61.43.Dq

1. INTRODUCTION

The III-V nitrides are very promising systems for optoelectronic applications in the blue and ultraviolet wavelengths and recently as high-power, high-temperature semiconductor elements with more elastic electronic properties than other semiconductor materials [1-3]. The wurzite crystalline structures of AlN, GaN, and InN have direct room temperature band gaps equal to 6.2, 3.4, and 1.9 eV, respectively, and form ternary alloy systems over the whole alloy composition range from x=0 to x=1. These properties place nitrides, and particularly the $Ga_{1\_x}Al_xN$ alloys of this group, at the very front of basic research and application tasks. Thus, analysis of the crystalline structure and local crystalline order is of pertinence today. The crystal morphology and the crystalline structure of bulk and epitaxial thin films of $Ga_{1\_x}Al_xN$ have been meticulously studied [1-3] and extended x-ray absorption fine structure (EXAFS) analysis have been performed [4]. The EXAFS technique [5] yields valuable information as to bond lengths and distances between first or nearest-neighbor (NN) ions Ga_N, and second or next-nearest neighbor (NNN) ions Ga–Ga and Ga–Al.

2. GENERALITIES

The characteristic structural coordination of an ideal zincblende or wurzite tetrahedron of a binary compound for the first two coordination shells is that around the central anion (cation) there are four cations (anions) in the first (NN) shell and twelve anions (cations) in the second (NNN) shell. In an ideal wurzite the inter-atom topology of the first two shells is identical to that of a zincblende crystal structure [1 vol.57]. It is beyond the second shell that the two structures differ because the adjacent tetrahedra of wurzite are rotated 120° around the common anion-cation-anion direction, thus resulting in hexagonal (wurzite) crystals with two distinct basic crystal lattice constants a and c with, for the ideal case, c/a=1.633 [1,6]. Thus, for an analysis limited to the first two shells, the conclusions of the zincblende local structure model are applicable to wurzite structures without limitation. To express the dimensions and angles of a regular tetrahedron of any basic, ideal face centered cube (f.c.c.) and wurzite structures is a simple trigonometric task.

The situation is more complex for ternary $A_xB_{1\_x}Z$ compounds. As mentioned above, in tetrahedral coordination each anion is surrounded by four cations, and vice versa. For ternary $A_xB_{1\_x}Z$ type compounds, (Fig. 1), A cations are replaced successively by B cations and give rise to five different elemental tetrahedra of which, content-wise, two are binary AZ and BZ, signed respectively T_0 and T_4, and three ternary T_1, T_2, and T_3, with one, two, and three A ions replaced by B ions [7]. In the case of a random distribution, the probabilities of the five configurations are described by Bernoulli binomials [8]. However, ternary [7,9] and quaternary [10] compounds generally exhibit preferences that result in site occupation preferences (SOPs) [7,9,10]. For that we developed the *strained tetrahedron* model [7].

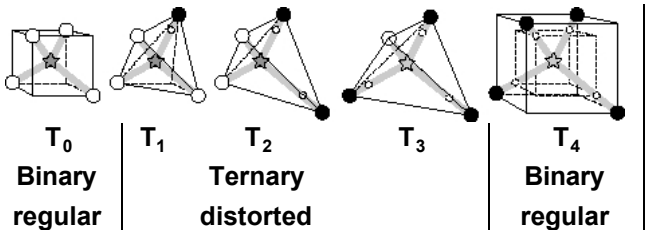

Fig.1 Aspect of the five elemental tetrahedron configurations $\{T_k\}_{k=0,4}$ of ABZ (or AYZ) ternary alloys. Small open circles indicate the would-be ion-positions as per *rigid tetrahedron* hypothesis.

3. THE MODEL

The model is based on the following seven axioms: *1)* The elemental tetrahedra are free to have different sizes and shapes (see Fig.1 and [7]). *2)* Bernoulli binomial polynomials with preference weight coefficients describe ion-pair and configuration probabilities. *3)* All NNN and higher shell fills are determined by the three NN SOP coefficients (W_1,W_2,W_3). *4)* As dilution varies, the total coordination-number conservation limits the range of values with physical meaning to ($0 \le W_1 \le 4$, $0 \le W_2 \le 2$, $0 \le W_3 \le 4/3$). *5)* The formation of each ternary configuration proceeds, complying with stoichiometry and mass conservation, until *full consumption of one of the binary ingredients*, or of both simultaneously as in the random case. *6)* All nineteen elemental inter-ion ternary distances are tetrahedron-constrained. 7) The elemental volumes of the two sublattices, for each of the three strictly ternary configurations, relax pair-by-pair to common values (leading to three volume relaxation constraints on the inter-ion distance parameters).

Through the unfolding of EXAFS data, for ideal tetrahedron coordinated zincblende and wurzite structures, the model characterizes the crystals in size, shape, and in their ion site preference occupation (with respect to random distributions) [7].

4. GaAlN ANALYSIS

GaAlN binary components, AlN and GaN, both have slightly distorted wurzite structures with their ***c/a***= 1.601 and 1.626 respectively [6], i.e., deviating from the ***ideal wurzite*** structure [1,6]. Consequently, their $Ga_{1\_x}Al_xN$ alloys will also reflect the original distortions of the binary constituents. These deviations, as well as the lattice mismatch of the sapphire substrate with the superimposed epitaxial layer of GaAlN, create additional internal stresses. A random distribution of the ion constituents of ternary compounds tacitly implies that the standard enthalpies of creation ($\Delta_f H_0$) of the component binaries are equal, and that SOP coefficients $W_1=W_2=W_3=1$. However, the $\Delta_f H_0$ of GaN and AlN binary compounds are, respectively, _76 > _110.5 [kJ/mol] [11,12]. We thus expect strong site occupation preferences in GaAlN, as previously observed for several other ternary compounds [9]. To check this suggestion, the deviations being small, we applied the statistical *strained-tetrahedron* model [7,9] to analyze the $Ga_{1\_x}Al_xN$ EXAFS data of Miyano & al. [4]. The reported Gallium K_edge EXAFS experimental data are analyzed for five $Ga_{1\_x}Al_xN$ alloy compositions with x={0, 0.158, 0.273, 0.333, 0.438} relative Al-content (x_{Al}). Miyano & al [4] report that the average values of lattice constants ***a*** and ***c*** for the alloy exhibit approximately a linear dependence.

We report graphically the data relative to the average of the second-neighbor NNN coordination numbers $<^{GaGa}CN(x)>$ (in EXAFS analysis a coordination number is usually signed Ni, but our statistical approach uses the more convenient mnemonic "CN" notation [6]) and $<^{GaAl}CN(x)>$, as well as inter-ion distances of NN $<^{GaN}d(x)>$ and of NNN $<^{GaGa}d(x)>$ and $<^{GaAl}d(x)>$. The values and uncertainties are read from the reported plots, which somewhat handicaps the accuracy of the input data. The data as read-in are shown as points and error bars in the figures.

The strained-tetrahedron model [7] is used to unfold the available $<^{GaGa}CN(x)>$ and

$<^{GaAl}CN(x)>$ data and, for the three SOP-coefficient values, yields {W_1, W_2, W_3}={0, 1.87, 1.00}. This fully determines all the probability distributions as well as all eight $<^{ij}CN(x)>$ curves,

where ij={GaN, AlN, GaGa, GaAl, AlGa, AlAl, $N_{Ga}N$, $N_{Al}N$}.The simultaneous availability of $<^{GaN}d(x)>$, $<^{GaAl}d(x)>$, and $<^{GaGa}d(x)>$ data for four x-values allows the definition of all T_2 and T_3 sizes and shapes [7], as summarized in Table 1.

TAB. 1: Complete $Ga_{1-x}Al_xN$ set of SOP coefficients, distances, angles, and volumes determined by the model for the ideal, allowed, elemental configuration tetrahedra. Bold: results of unfolding. *Italics*: values derived from unfolded data; binary values from Miyano & al. [4] data.

Confi-guration	k	W_k	$^{AlN}d_k$	$^{GaN}d_k$	$^{AlAl}d_k$	$^{GaGa}d_k$ [Å]	$^{GaAl}d_k$	$^{NAlN}d_k$	$^{NGaN}d_k$	α_{AlNAl}	α_{GaNGa} [°]	α_{AlNGa}	Vol [Å^3]
T_0	0	1	-	1.950	-	3.184	**-**	**-**	3.184	-	109.47	-	3.81
T_1	1	**0**	**-**	**-**	**-**	**-**	**-**	**-**	**-**	**-**	**-**	**-**	-
T_2	2	**1.87**	*2.32*	**1.61**	*3.44*	**2.96**	**3.15**	*3.79*	*2.63*	*95.5*	*134.2*	*105.2*	*2.99*
T_3	3	**1.00**	*1.80*	**2.10**	*2.98*	**-**	**3.13**	*2.93*	*3.42*	*112.0*	*96.6*	*106.8*	*3.41*
T_4	4	1	1.894	-	3.092	-	-	3.092	-	109.47	-	-	3.49

Indeed, by unfolding the reported $<^{ij}d(x)>$ variations we get the corresponding elemental distances $\{^{GaN}d_k, ^{GaGa}d_k, ^{GaAl}d_k\}_{k=2,3}$, while distances related to the non-reported variations $\{^{AlN}d_2, ^{AlAl}d_2, ^{AlN}d_3, ^{AlAl}d_3\}$ are derived from the unfolded values using the *tetrahedron-symmetry constraints,* and the two-lattice *volume relaxation constraint* [7]. Once we know all the elemental distance $\{^{ij}d_k\}$-values, we can determine the angular and remaining tetrahedron values (Table 1), as well as all seven $<^{ij}d(x)>$ curves: $<^{GaN}d(x)>$, $<^{AlN}d(x)>$, $<^{GaGa}d(x)>$, $<^{GaAl}d(x)>$, $<^{NGaN}d(x)>$, $<^{AlAl}d(x)>$, and $<^{NAlN}d(x)>$. The resulting sizes and shapes of allowed T_k configurations are given in Table 1. Once more we remind the reader that the "ternary" values written in "bold" correspond to the direct results of the unfolding, assuming that the wurzite crystal be ideal; the results in "italics" are derived from the values in bold**,** assuming strained but symmetric tetrahedra. Therefore, these results should be taken as indicative until more accurate values become available.

We present graphically a) the average coordination numbers (Fig.2); b) the corresponding deformed (with respect to random) configuration probabilities (Fig.3); c) the average inter-ion distances (Fig.4). To illustrate the accuracy of the model, the original published EXAFS points are superimposed on the model curves.

Assuming the VCA curves to be reasonably close to the corresponding Vegard lines (well defined for both NN and NNN), from the measured GaN-points, we derived the expected AlN "transpose-points" (open-rhombi) in Fig.4; these perfectly overlap the calculated $<^{AlN}d(x)>$-curve. All seven curves and available experimental points are given in Fig.4.

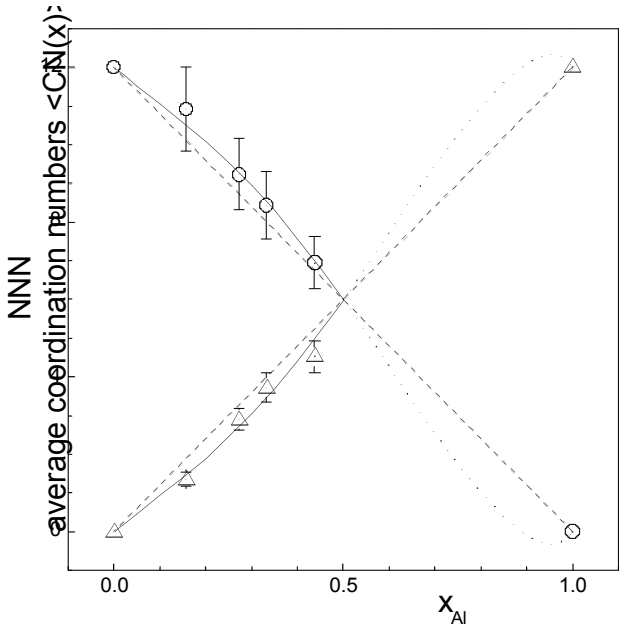

FIG.2 NNN coordination-numbers: experimental [4] $<^{GaGa}CN(x)>$ _, $<^{GaAl}CN(x)>$ **Δ** values with error bars, and model curves vs. $x=x_{Al}$ (solid curves for $x_{Al}\leq 0.5$, then dotted as the crystal becomes inhomogeneous). Dashed lines: random case reference.

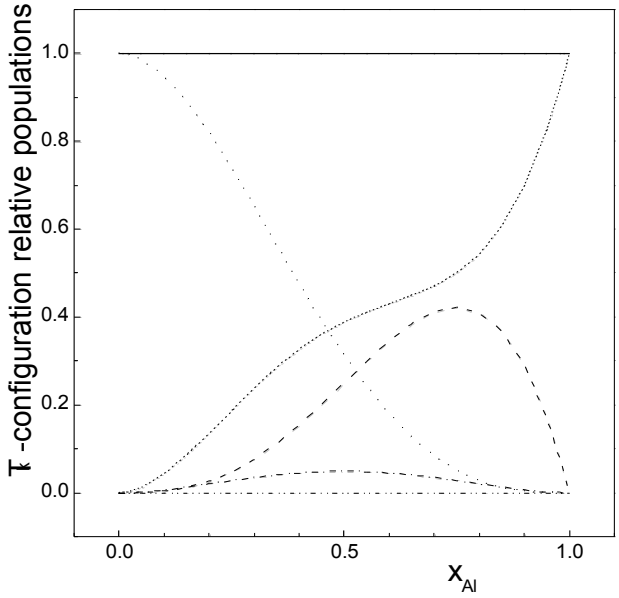

FIG.3 Population probabilities $P_k(x)$ for the five T_k configurations vs. $x=x_{Al}$ content: **a)** $P_0(x)$ dotted; **b)** $P_1(x)$ dot-dot-dash; **c)** $P_2(x)$ dot-dash; **d)** $P_3(x)$ dash; **e)** $P_4(x)$ thin short dash; **f)** $\Sigma\ P_k(x)$ thick straight solid curves.

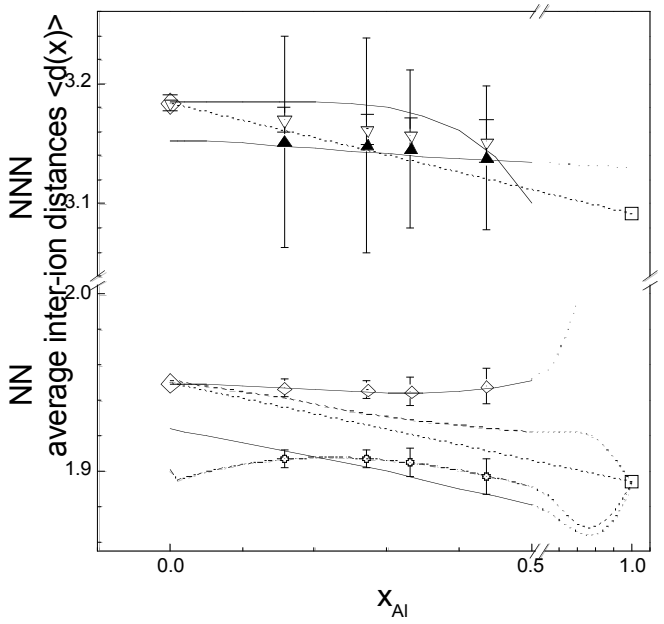

FIG.4 Inter-ion <d(x)> curves vs. x=$x_{Al.}$ Model-derived (thick solid curves for x≤0.5, then dotted as crystal turns inhomogeneous) and experimental [4] values with their error bars: **a)** $<^{GaN}d(x)>$ ◊; **b)** $<^{AlN}d(x)>$ **o** AlN "transpose" of the measured GaN-points; **c)** $<^{GaGa}d(x)>$ _; d) $<^{GaAl}d(x)>$ _. _GaN; _AlN data from the literature [11]. For reference NN and NNN Vegard (straight dashed lines); unreported <d(x)> trend model-estimation (dot-dash lines).

5. DISCUSSION

Random distribution corresponds to the highest level of population probabilities of the three "ternary" configurations T_1, T_2, and T_3. Any departure from such a distribution ($W_k \neq 1$) leads to a decrease in the corresponding configuration probability, to the benefit of one of the binary tetrahedra T_0 (if $W_k<1$) or T_4 (if $W_k>1$) [7,13]. This redistribution takes place within the binary constituent tetrahedra and leads to NO clustering whatsoever, with the spatial distribution remaining perfectly random.

The fact that $W_1=0$ for GaAlN alloys implies that the creation of the T_1 configuration is forbidden in GaAlN. This, together with a value of $W_2=1.87$ close to (yet NOT equal to) its limit =2 (see axiom 4), leads to strongly deformed (with respect to random) probability distributions with two heavily predominant "binary" T_0 and T_4, both highly enhanced, and a nearly sole "ternary" T_3 configuration (see Fig.3). Indeed, up to about x=0.5, all the configurations have monotonic probability variations $\{P_k(x)\}_{k=0,4}$: $P_0(x)$ remains dominant for x<0.45, decreasing from [1→0.31], while increasing from zero are $P_4(x)$ [0→0.39] dominant throughout over $P_3(x)$ [0→0.25] and $P_2(x)$ [0→0.05]. The last two cross over at x≈0.15 $P_3(x) < P_2(x) < 0.015$. With $W_2=1.82$ and $P_2(x)<5\%$ (of the total content), the accuracy of the T_2-related values may suffer.

Although with a highly attenuated probability, it is the T_2-tetrahedra that allow the wurzite crystal to develop a homogeneous linking-together of T_0 and T_4 tetrahedra. Beyond x=0.5, T_2 concentration drops to a point where the "linking" becomes uncertain and crystals develop "inhomogeneously". For clarity, consider the topological nature of T_2 tetrahedra, with two A atoms and two B atoms. Such tetrahedra allow a fully homogeneous growth of the crystals, by linking together regular binary T_0 and T_4, as well as distorted T_1 (absent in GaAlN) and T_3-type

tetrahedra. Observing the small value and decrease in the T_2 type population probabilities shown on Fig.3, we expect a decrease in the homogeneity of the GaAlN alloy beyond a 50% content of Al. Another important foreseen consequence of the large SOP departure from a random distribution is [14,15], the decrease in the number of GaAlN far IR phonon components from eight lines to four strong and two weak (≈≤5% intensity) lines.

6. CONCLUSION

In this paper we have used the *strained-tetrahedron* model to analyze the wurzite structure of epitaxial GaAlN thin films on a sapphire substrate [7,9]. The three SOP coefficients and NN and NNN inter-ion distances are calculated in the ideal wurzite structure approximation. A strong deviation from random distribution is observed with W_1=0, W_2=1.86, and W_3=1, with Ga-N pairs strongly preferred to Al-N pairs. This confirms the correlation of pair-preferences with the lower $\Delta_f H_0$ standard enthalpy of creation, as commented on in [9]. A final consideration of SOP analysis suggests that from a thermodynamic point of view the wurzite structure of epitaxial GaAlN thin films could be less homogeneous and more difficult to grow above 50% AlN content in GaAlN.

ACKNOWLEDGEMENTS

Part of the work was supported by the EU TARI-project contract HPRI-CT-1999-00088

REFERENCES

(1) Ed.s J.I.Pankove, Th.D.Moustakas, *Gallium Nitride (GaN) I,* Semiconductor and semimetals, vol.**50**, Academic Press, London, 1998; *idem, Gallium Nitride (GaN) II*, vol.**57**, 1999
(2) J.S.Blakemore, *J.Appl.Phys*. **53** R123 (1982)
(3) H.Morkoç, S.Strite, G.B.Gao, M.E.Lin, B.Sverdlov, M.Burns, *J. Appl. Phys*., **76**, 1381 (1994)
(4) K.E.Miyano, J.C.Woicik, L.H.Robins, C.E.Bouldin, D.K.Wickenden, *Appl. Phys. Lett*. **70**, 2108-10 (1997)
(5) P.A. Lee, P.H. Citrin, P. Eisenberger, B.M. Kincald, *Rev. Mod.Phys*., **53**, 769 (1981); A.F.Wright, J.S.Nelson, *Phys.Rev.B* **51** 7866 (1995)
(6) A.F.Wright, J.S.Nelson, *Phys.Rev.B* **51** 7866 (1995)
(7) B.V.Robouch, A.Kisiel, J.Konior, *J. Alloys Compounds* **339**, 1 (2002)
(8) Balzarotti, N. Motta, A. Kisiel., M. Zimnal-Starnawska, M.T. Czyzyk, M. Podgorny, Rhys. Rev. B 31, 7526 (1985)
(9) B.V.Robouch, A.Kisiel, J.Konior, *J .Alloys Compounds* **340**, 13 (2002)
(10) B.V.Robouch, A.Kisiel, *Acta Phys.Pol.A* **94** 497 (1998); idem: *J. Alloys Compounds* **286** 80 (1999)
(11) Landolft-Börnstein, vol. **17** *Semiconductors*, Ed. K.-H. Hellwege, Springer Verlag, Berlin 1982
(12) Lange's Handbook of Chemistry, Ed. J.A.Dean, 14th edition, McGraw Hill Inc., New York 1992.
(13) B.V.Robouch, E.Burattini, A.Kisiel, A.L.Suvorov, A.G.Zaluzhnyi, *J. Alloys Compounds* **359**, 73-78 (2003)
(14) B.V.Robouch, E.M.Sheregii, J.Polit, J.Cebulski, E.Burattini, *Fiz. Nizkikh Temp: Low Temp. Phys*. **30**, 1225 (2004)
(15) B.V.Robouch, E.M.Sheregii, A.Kisiel, *phys .stat. sol*. (2003) (*in press*)